Clays and Clay Minerals, Vol. 46, No. 1, 63–68, 1998.

CHARACTERIZATION OF INTERCALATED SMECTITES USING XRD PROFILE ANALYSIS IN THE LOW-ANGLE REGION

DANIEL JANEBA,[1] PAVLA ČAPKOVÁ,[1] ZDENĚK WEISS[2] AND HENK SCHENK[3]

[1] Faculty of Mathematics and Physics, Charles University Prague, Ke Karlovu 5, 121 16 Prague, Czech Republic

[2] Central Analytical Laboratory, Technical University of Mining and Metallurgy, 708 33 Ostrava, Czech Republic

[3] Laboratory of Crystallography, University of Amsterdam, Nieuwe Achtergracht 166, 1018 WV Amsterdam, The Netherlands

Abstract—X-ray diffraction (XRD) characterization of natural and intercalated smectites is usually limited to the apparent *d*-value estimated from the peak maxima in the raw data. This can lead to the misinterpretation of the measured data. In the case of XRD, the interference function is modulated by instrumental factors (Lorentz-polarization factor, diffraction geometry) and physical factors (structure factor, surface roughness effect). These effects lead to diffraction profile distortions, depending on the diffraction angle and peak full width at half maximum (FWHM). As a result, the diffraction profiles for structures with large line broadening (FWHM $> 1°$) exhibit a significant peak shift ($\Delta d \sim 1.5$ Å), especially at low angles ($2\theta \leq 10°$). The present work deals with the detailed analysis of all these effects, their corrections and their consequences for the interpretation of diffraction patterns (including possible errors in determining lattice parameters or the structure model). The investigated materials were montmorillonites (MMT) intercalated with hydroxy-Al polymers. Diffraction profile analysis revealed the corrected *d*-values and showed that the intercalated sample is not a mixed-layered structure. As a result a structural model of the interlayer is presented.

Key Words—Montmorillonite, Profile Analysis, Smectite, XRD.

INTRODUCTION

The search for highly efficient sorbents and catalysts has led to the development of 2-dimensional molecular sieve-type materials based on clays. These new classes of materials, known as pillared interlayer clays (PILC), are generally prepared by intercalation of smectites with inorganic polymeric cations (Mitchell 1990). The technology of PILC synthesis requires careful monitoring based on the accurate and reliable characterization of prepared material. X-ray diffraction (XRD) characterization of original and pillared montmorillonites presented in the literature is usually limited to the apparent *d*-values estimated from the peak maxima in the raw data (Figueras et al. 1990; Hsu 1992). It will be shown that this method of analysis can lead to misinterpretations of measured data. For structures exhibiting diffraction line broadening, the low-angle region of a diffraction pattern shows certain characteristic distortions arising from instrumental factors such as Lorentz-polarization factor or the diffraction geometry and physical factors such as the structure factor or the surface roughness effect. The distortions are a continuous function of diffraction angle, regardless of the cause of the line broadening. This work analyzes these effects and discusses potential consequences for interpretation of diffraction patterns such as the incorrect determination of lattice parameters or possible incorrect conclusions concerning structural disorder or phase identification. A method to determine the *d*-value of basal planes in the montmorillonite structure (that is, determination of the lattice parameter *c*) is given. This method of profile analysis can also help to determine the phase composition of intercalated smectite (that is, to distinguish an interstratified structure with an irregular mixing of layers of 2 different *d*-values corresponding to the intercalated and nonintercalated smectites from a mixture of 2 segregated phases, intercalated and nonintercalated).

THEORY

Turbostratic arrangements of silicate layers in certain clay minerals, notably in those of the smectite group, strongly affect the diffraction pattern. Consequently the powder diffraction pattern shows mainly basal (00*l*) reflections and 2-dimensional *hk* diffraction bands. These *hk* bands are not well suited to structure analysis, and the identification and characterization of intercalated clays is mainly based on the basal reflections. The (00*l*) line broadening may be caused by distortion of the silicate layers, by small particle size and by irregular mixing of layers of different basal spacings in the layer stacking. Moreover, the intensities are reduced by thermal motion. As a result of all these effects, only 2 or 3 basal reflections are usually observable and the information contained in the diffraction pattern is very limited. The present work deals with profile analysis of the (00*l*) series.

The integrated intensity I_{001} and profile intensity $I(2\theta)$ of basal (00*l*) reflections are (in case of powder sample) given by:

$$I_{00l} = S\ Lp|F|^2_{001}A \quad [1]$$

$$I(2\theta) = S\ Lp|F|^2A\Phi \quad [2]$$

where S is a scale, Lp is the Lorentz polarization factor, $|F|^2_{00l}$ is the structure factor squared, A is an absorption factor (representing the volume absorption, surface absorption and the absorption in the sample holder) and Φ is the profile interference function. In the case of narrow diffraction lines we can assume that the angle-dependent terms (Lp, $|F|^2$, A) do not change across the line width and therefore the line position can be taken as the position of maximum intensity. If the diffraction profiles are broadened, the angle dependence of these factors must be taken into account (Reynolds 1980). The considerable change of the line profiles, and the consequent shift of the peak maxima to lower 2θ, have been observed after the correction of experimental diffraction diagrams for these angle-dependent factors (Lp, $|F|^2$, A). These changes stimulated us to a more detailed investigation of these effects.

Effects Leading To Diffraction Profile Distortions

LORENTZ-POLARIZATION FACTOR. The Lorentz-polarization correction for Bragg–Brentano geometry (without a monochromator) is given by (see Klug and Alexander 1974):

$$Lp = \frac{1 + \cos^2 2\theta}{2 \sin^2 \theta \cos \theta} \quad [3]$$

STRUCTURE FACTOR. The angular dependency of structure factor is given by:

$$F(2\theta) = \sum_{j=1}^{N} n_j f_j\left(\frac{\sin\theta}{\lambda}\right)\cos\left(\frac{4\pi z_j \sin\theta}{\lambda}\right) + i\sum_{j=1}^{N} n_j f_j\left(\frac{\sin\theta}{\lambda}\right)\sin\left(\frac{4\pi z_j \sin\theta}{\lambda}\right) \quad [4]$$

where λ is the wavelength, n_j is the number of atoms of each type in unit cell in positions z_j (in Å), f_j is the atomic scattering amplitudes which can be calculated using the coefficients for analytical approximation to the scattering factors:

$$f\left(\frac{\sin\theta}{\lambda}\right) = \sum_{j=1}^{4} a_i \exp\left[-b_i\left(\frac{\sin\theta}{\lambda}\right)^2\right] + c \quad [5]$$

and a_i, b_i, c are the coefficients taken from Ibers and Hamilton (1974).

VOLUME ABSORPTION. The volume absorption for the symmetrical Bragg–Brentano geometry and thick sample ($t \rightarrow \infty$, where t is the thickness) is:

$$A = \frac{1}{2\mu} \quad [6]$$

where μ is the absorption coefficient. This kind of absorption is angular independent and does not contribute to the angular dependent corrections for thick sample.

THE LOW-ANGLE DIFFRACTION GEOMETRY. As the interplanar spacing of intercalated smectites is between 15 and 20 Å, the diffraction angles for (001) and (002) peaks are very low ($2\theta < 12°$). Diffraction peaks at such low angles are affected much more by the instrumental and physical factors than the peaks at higher diffraction angles and that is why more attention should be paid to their detailed analysis.

Surface Roughness Effect. There is strong absorption by the rough surface of the sample which affects especially the intensity of diffraction peaks at lower 2θ angles. If the surface is modeled as a surface with cubes upon it, the radiation has to pass the cube before reaching the detector and the intensity (Berg and Wachters, personal communication 1992) is:

$$I(\alpha, \beta) = I(90°, 90°)[1 - \epsilon(\cot\alpha + \cot\beta)] \quad [7]$$

$$\epsilon = Nd^2[1 - \exp(-\mu d)] \quad [8]$$

where N is the number of cubes per unit area, d is the edge of the cube, $\alpha, \beta \leq 90°$, $\alpha + \beta = 2\theta$, α is the angle between the incident beam and the surface of the sample, β is the angle between the diffracted beam and the surface of the sample and μ is the absorption coefficient.

The Primary Beam Intensity. At low angles the trace of the primary beam is very large, even larger than the area of the sample, and part of the primary beam irradiates the sample holder. At higher angles the trace is getting smaller and the whole primary beam irradiates only the sample. At Bragg–Brentano geometry the change of the trace of the primary beam is given by:

$$1/\sin\theta \quad [9]$$

This effect can be replaced when using the automatic divergence slit.

The Absorption Of The Sample Holder. Part of the diffracted beam is absorbed by the sample holder which also affects the diffraction profile.

EXPERIMENTAL

X-ray powder diffraction diagrams were obtained using a Philips powder diffractometer with a vertical goniometer, using Cu*K*α radiation and a Ni filter. A step size of 0.02° in 2θ and a measuring time of 20 s per step were used to record the diffraction pattern. The divergence slit was ½°, and 0.1 mm scatter and receiving slit were used. The radius of the goniometer was 17 cm.

As the flat sample holder is in the horizontal position during the measurement, powder can be pressed into the sample holder without any binding agent. The

https://doi.org/10.1346/CCMN.1998.0460107 Published online by Cambridge University Press

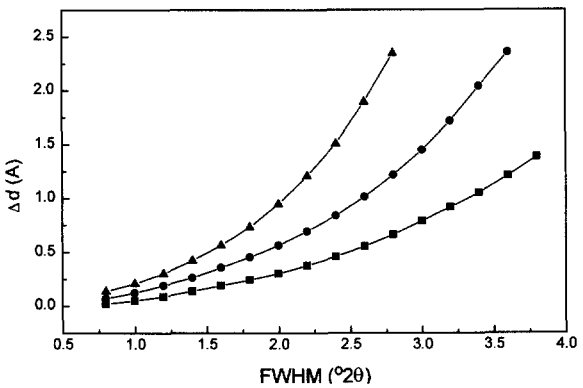

Figure 1. Magnitude of the peak shift Δd after the Lp correction for 3 different d-values as a function of peak width for Cu$K\alpha$ (d = 18 Å, triangles; d = 15.2 Å, circles; d = 12.5 Å, squares).

samples prepared in this fashion show 00l preferred orientation.

Natural Na-MMT was intercalated in an aqueous solution in which Na^+ ions were replaced by Al-hydroxy complexes. The intercalated sample contained 25% Na-MMT as determined by chemical analysis.

Chemical analysis showed 2.66 Al atoms in interlayer per unit cell corresponding to either Keggin 5+ ions $[Al_{13}O_4(OH)_{26}(H_2O)_{10}]^{5+}$ (described by Johansson 1962) or to gibbsite-type double-ring sandwiches $[Al_{20}(OH)_{54}(H_2O)_{22}]^{6+}$. For structure models see Čapková et al. (1998). Computer simulations (CERIUS^2) gave the same d-values [d(001) = 19.6 Å] for both (Čapková et al. 1998).

We assumed that the structure of clay sheet did not change during the process of intercalation.

RESULT AND DISCUSSION

The above-described corrections were investigated and then applied to the measured diffractogram of intercalated montmorillonite. Each of the effects (instrumental or physical) is expressed by a mathematical function that modifies the interference function. All of the described effects represent multiplicative influences to the profile function. To obtain the profile function it is necessary to correct the measured data using the described correcting functions. This operation leads to a change in the shape of the profile and the peak positions may be shifted. The magnitude of the shift of peak positions is proportional to the FWHM of the peak and also to the d-value, and the direction of the shift depends on the behavior of the correcting function. Strictly speaking, the magnitude of the shift is given by the first derivative of the correcting function and the direction of the peak shift depends on the sign of the first derivative of the correcting function. For example, steeply decreasing Lp dependence shifts the peak position to higher 2θ angles. Also, the magnitude of the peak shift is higher for peaks with larger FWHM and for peaks at lower diffraction angles. Specific examples are discussed below.

The Lorentz-Polarization Factor

We calculated peak position shifts caused by the Lorentz-polarization factor for different FWHMs for 3 different peaks. Diffraction profiles were simulated (Rafaja 1988) for different particle sizes and different values of microstrain, and the correction for the Lorentz-polarization factor was carried out. The peak position shifts are shown in Figure 1. It can be seen that the shift is much more significant for lower diffraction angles and higher FWHM. This is exactly the case of intercalated smectites where the (001) line corresponds to d-values between 15 and 20 Å and is broadened (see above).

The Structure Factor

A knowledge of the structure model is necessary for the structure factor correction. There are large differences in angular dependencies of the structure factor for different types of Al-hydroxy cations. Two cations were assumed in the interlayer: the Keggin 5+ and gibbsite-like double-ring sandwich. The structure factor calculations used structural models from molecular simulations as reported by Čapková et al. (1998).

As the angular dependence of the square of structure factor for montmorillonite intercalated with Al-hydroxy polymers is not monotonic, the diffraction peaks (001) and (002) can be shifted in opposite directions depending on the sign of the derivative of the structure factor curve: if the sign of derivative is negative, the peak position is shifted to higher angles, as in the case of Lorentz-polarization factor, whereas if the sign of the derivative of the correcting function is positive, the peak position is shifted to lower angles.

The angular dependences of the square of the structure factor for Na-MMT, MMT intercalated with Keggin 5+ and MMT intercalated with gibbsite-like double-ring sandwiches are shown in Figure 2.

The Low-Angle Diffraction Geometry

To get reasonable results, it is necessary to take into account the specific features of the low-angle geometry, as follows.

THE ABSORPTION OF THE SAMPLE HOLDER. The sample was placed in a square-shaped plastic holder (see Figure 3). Part of the diffracted radiation is absorbed by the holder so the irradiated volume of sample is not equal to the volume from which the diffracted radiation is detected. The diffracting volume for Bragg–Brentano geometry is in the shape of a prism with a triangular base and the volume is proportional to tan θ.

THE SURFACE ROUGHNESS EFFECT. To get a correcting function describing the surface roughness effect, we

https://doi.org/10.1346/CCMN.1998.0460107 Published online by Cambridge University Press

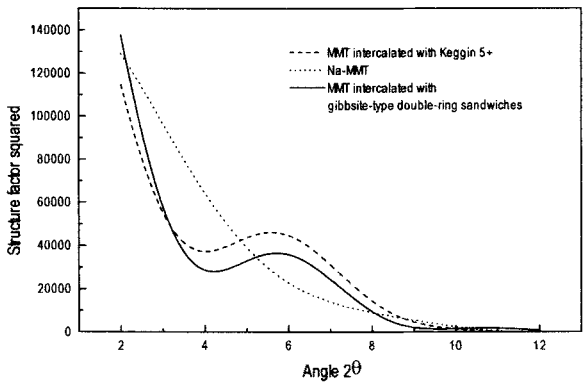

Figure 2. The angular dependences of the structure factor for MMT (Na-MMT, MMT intercalated with Keggin 5+ cation and MMT intercalated with gibbsite-type double-ring sandwich). The concentration of Al is 2.66 atoms per unit interlayer.

assumed that we are dealing with an ideal rough surface. For such a surface, half of the surface area is covered by cubes. The absorption coefficient for AL-MMT is $\mu = 52.2\ cm^{-1}$ (the value was calculated according to the chemical composition). The cube edge was assumed to be $d = 5\ \mu m$, which is the edge of the cubic grains of our sample. Then the intensity I_{BB} for symmetrical Bragg–Brentano geometry (from Equations [7] and [8]) is given by:

$$I_{BB} = 1 - \cot\theta \qquad [10]$$

The Profile Analysis of Powder Diffractogram of Intercalated Montmorillonite

With all these corrections together, the detailed profile analysis of intercalated montmorillonite was made possible.

The measured diffractogram without any corrections and the diffractogram corrected for the Lp factor are shown in Figure 4. Many authors use the raw data or the Lp-corrected diagram for lattice parameters estimation which might cause the differences in d-values published in literature. The corresponding d-values are included in Table 1. The peaks were located using the computer program Difpatan (Kužel 1990). The misfit of the d-values indicates that the more detailed profile analysis is necessary. Our aim was to obtain an interference function that is not affected by any instrumental or physical factors and which can give the most accurate information about the d-values. To obtain the interference function, the above-discussed effects were taken into account and the correcting functions were taken as indicated above: Equation [3] for Lorentz-polarization factor, Equation [4] for the square of the structure factor, Equation [9] for the primary beam intensity and Equation [10] for the surface roughness effect. The absorption in the sample holder was taken

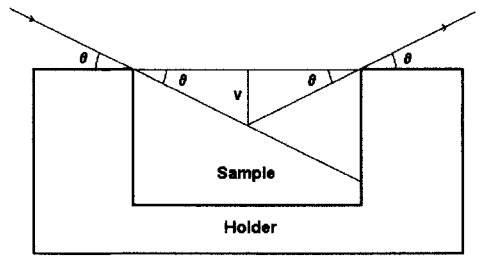

Figure 3. The absorption of sample holder for Bragg–Brentano geometry: the actual diffracting volume is a prism with a triangular base, v is the depth of penetration, θ is the diffraction angle.

to be dependent on tan θ, and the volume absorption was taken to be angular independent.

The correction for the square of the structure factor was done for both models of the interlayer, that is, for the Keggin 5+ cation and for the gibbsite-type double-ring sandwich (Figure 5). We obtained an "impossi-

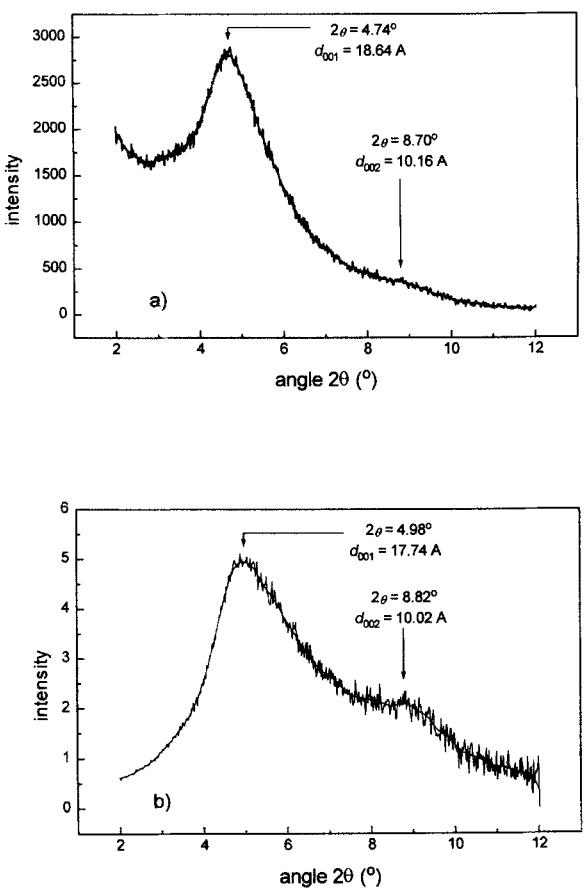

Figure 4. a) Measured profile of MMT intercalated with gibbsite-type double-ring sandwich (concentration 2.66 Al atoms per unit interlayer, Bragg–Brentano geometry); b) profile of MMT intercalated with gibbsite-type double-ring sandwich after the Lorentz-polarization factor correction.

https://doi.org/10.1346/CCMN.1998.0460107 Published online by Cambridge University Press

Table 1. Diffraction line positions and corresponding d-values for (001) and (002) line of intercalated MMT in raw data and after corrections.

	(001)		(002)	
	Position (°2θ)	d(001) (Å)	Position (°2θ)	2d(002) (Å)
Measured profile	4.74	18.64	8.70	20.33
Lp-corrected profile	4.98	17.74	8.82	20.05
Interference function for gibbsite-type double-ring sandwich (Na-MMT included)	4.59	19.25	9.30	19.02
Interference function for gibbsite-type double-ring sandwich (Na-MMT not included)	4.45	19.86	9.30	19.02
Simulated interference function for mixed structure 75% Al-MMT + 25% Na-MMT	4.75	18.60	8.85	19.98

ble" interference function from the correction for Keggin 5+ cation with an artificial peak which does not have any physical meaning and indicates an incorrect structural model of the interlayer. In addition ^{27}Al NMR spectroscopy did not indicate the tetrahedral coordination of Al typical for Keggin cations. In contrast, the peak positions for the gibbsite-type double-ring sandwich correction fit perfectly with the computer simulations. Moreover, the d(001) and 2d(002) are very similar to each other (they are in the range of errors estimated as 0.2 Å). This is in the case when 25% of Na-MMT is included in the structure factor calculation (d-values in Table 1), as the chemical analysis showed 25% of nonintercalated Na-MMT. The presence of a nonintercalated Na-MMT causes a strong asymmetry of the (001) peak as seen in Figure 4. The resulting interference function (after all corrections) for MMT intercalated with gibbsite-type double-ring sandwiches is shown in Figure 6.

The peak positions and profiles of the interference function were compared with the calculated peak positions and profiles of the interference function of a 2-phase Al-MMT + Na-MMT sample [d(001) = 19.5 Å, d(001) = 12.5 Å] and with peak positions and profiles simulated for a mixed structure [75% Al-MMT with d(001) = 19.5 Å and 25% Na-MMT with d(001) = 12.5 Å] (using formulas from Seul and Torney 1989). The peak positions of the measured interference function match with the calculated positions for a 2-phase sample, but not with the peak positions for a mixed-layered structure (Table 1). Consequently, we can conclude that there is no evidence that this sample is a mixed structure.

The interference function was simulated using the computer program Simul (Rafaja 1988) for different particle sizes and for different values of microstrain, and the simulated interference function was corrected in the opposite way using the same system of corrections (as used to correct the measured data). The aim was to get a diffraction profile similar to that which we measured. Good agreement was achieved for particle sizes 120 Å and microstrain $\Delta d/d$ = 0.01 for Al-MMT, and for particle size 150 Å and $\Delta d/d$ = 0.1 for the nonintercalated Na-MMT. The comparison of the calculated and measured profiles is in Figure 7.

CONCLUSIONS

Present results confirm that XRD profile analysis of clay minerals exhibiting diffraction line broadening

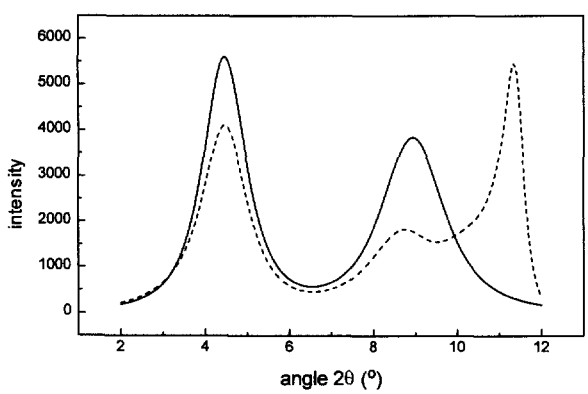

Figure 5. Correction for structure factor: solid line = data corrected for MMT intercalated with gibbsite-type double-ring sandwich; dashed line = data corrected for MMT intercalated with Keggin 5+ cation. The extra peak in the interference function indicates an incorrect structural model of interlayer.

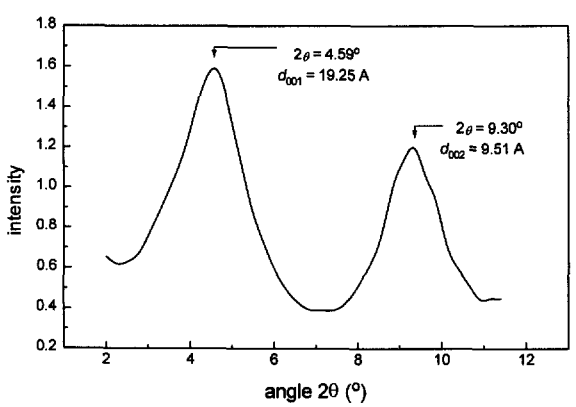

Figure 6. Resulting interference function for MMT intercalated with gibbsite-type double-ring sandwich, 25% of nonintercalated Na-MMT included in the structure factor.

https://doi.org/10.1346/CCMN.1998.0460107 Published online by Cambridge University Press

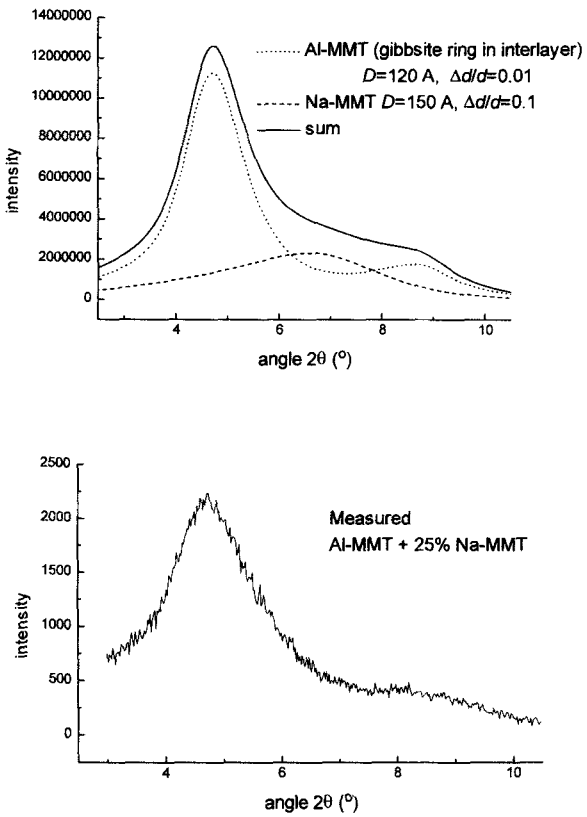

Figure 7. Calculated profile for a 2-phase sample (Al-MMT + Na-MMT) and measured profile (after background correction) of Al-MMT containing 25% of nonintercalated Na-MMT.

should include the corrections for all the angle-dependent factors in the intensity formula. For conclusions concerning the structural characteristics the consequences of neglecting these corrections were illustrated quantitatively. Lattice spacings may differ significantly from those corresponding to the raw data or to the Lp-corrected data. For a correct interpretation of diffraction data and a reliable conclusion about the structure, correction of the diffraction pattern is necessary.

This profile analysis can also detect an incorrect model as shown for the Keggin 5+ cation in the interlayer. This may occur because of different angular dependences of the square of the structure factor.

The shape of the corrected profiles (the shape of the interference function) yields additional information about the phase homogenity of the sample, which is especially interesting in the case of intercalation. The asymmetry of the (001) peak indicates that both forms, the Al intercalated MMT and the nonintercalated Na-MMT, are present in the sample. This conclusion is supported also by chemical analysis.

ACKNOWLEDGMENTS

This work was supported by the Grant Agency of the Czech Republic (205/94/0468), the Grant Agency of the Charles University (33) and by the US–Czechoslovak Science and Technology Joint Fund grant No. 93008. The authors are thankful to the crystallographers A. J. v. d. Berg and J. J. Wachters for submitting their work concerning surface roughness effect (personal communication, 1992).

REFERENCES

Čapková P, Driessen RAJ, Numan M, Schenk H, Weiss Z, Klika Z. 1998. Molecular simulations of the montmorillonite intercalated with aluminium complex cations. Parts I and II. Clays Clay Miner: in press.

Figueras F, Klapyta Z, Massiani P, Mountassir Z, Tichit D, Fajula F, Gueguen C, Bousquet J, Auroux A. 1990. Use of competetive ion exchange for intercalation of montmorillonite with hydroxy-aluminium species. Clays Clay Miner 38:257–264.

Hsu PH. 1992. Reaction of OH-Al polymers with smectites and vermiculites. Clays Clay Miner 40:300–305.

Ibers JA, Hamilton WC. 1974. International tables for X-ray crystallography, Vol. IV—Revised and supplementary tables. Birmingham: Kynoch Pr. 366 p.

Johansson G. 1962. The crystal structures of $[Al_2(OH)_2(H_2O)_8](SO_4)_2{\cdot}2H_2O$ and $[Al_2(OH)_2(H_2O)_8](SeO_4)_2{\cdot}2H_2O$. Acta Chem Scand 16:403–420.

Klug HP, Alexander LE. 1974. X-ray diffraction procedures for polycrystalline and amorphous materials. New York: Wiley Intersci Publ. 966 p.

Kužel R. 1990. Difpatan [computer program], Faculty of Math and Physics, Charles Univ, Prague, Czech Republic; available from kuzel@karlov.mff.cuni.cz.

Mitchell WI. 1990. Pillared layered structures. London: Elsevier. 252 p.

Rafaja D. 1988. Simul [computer program], Faculty of Math and Physics, Charles Univ, Prague, Czech Republic; available from rafaja@karlov.mff.cuni.cz.

Reynolds RC. 1980: Interstratified clay minerals. In: Brindley GW, Brown G, editors. Crystal structures of clay minerals and their X-ray identification. London: Mineral Soc.

Seul M, Torney DC. 1989. Statistical theory of X-ray scattering from crystals of finite size with pure displacement disorder in one dimension. Acta Crystallogr A45:381–396.

(Received 25 October 1996; accepted 30 April 1997; Ms. 2823)